Springer

KSME

Journal of Mechanical Science and Technology 24 (3) (2010) 671~679
www.springerlink.com/content/1738-494x
DOI 10.1007/s12206-009-1219-1

Reliability and fatigue life evaluation of railway axles †

Meral Bayraktar*, Necati Tahrali and Rahmi Guclu

Mechanical Engineering Department, Faculty of Mechanical Engineering, Yildiz Technical University, Istanbul, 34349, Turkey

(Manuscript Received February 6, 2009; Revised September 20, 2009; Accepted November 11, 2009)

Abstract

The axle is one of the most important components of a rail vehicle which transmits the weight of the vehicle to the wheels, meets the vertical and horizontal loads formed during static and dynamic moving, and carries the driving moment and braking moment. The prediction of fatigue failure of axles plays an important role in preventing fatigue fractures. Varying loads on components lead to cumulative failure in the mechanism. In this study, failures in axles of rail vehicles serving the Istanbul Transportation Co. have been investigated. Statistical evaluation of real life values has been performed by taking into account the kilometer and load cycle. Equivalent stresses have been used to derive life equations and diagrams by using one of the cumulative life theories known as the Palmgren-Miner method. Finally, theoretical and practical Wohler diagrams S-N (σ-N: stress-life) have been plotted to reveal error calculation.

Keywords: Cumulative fatigue damage; Fracture; Life; Reliability; Rail vehicle axle

1. Introduction

The development of railway systems has been an important driving force for technological progress. From the 1840s onward a dense railroad network spread all over Europe, America and other parts of the world. Within a few decades railways became the predominant traffic system carrying a steadily increasing volume of goods and number of passengers. This rapid development requires great responsibility for safety. A derailment in 1875 due to a broken wheel promoted the birth of the new research fields of fatigue. In 1848 James and Galton published results of tests on large iron bars subjected to alternating loads as there were known from railway axles. They show that the failure loads were lowered by up to two-thirds as compared to static loading in such cases. A few years later, German railway engineer August Wohler started his well known test series, the results of which were published between 1858 and 1871 [1]. In Fig. 1, the upper drawing shows Wohler's apparatus for the measurement of service strains on railway axles. The dashed line indicates the deflected position, and the below drawing shows Wohler's purpose-built fatigue testing machine to apply reserved bending to axle-like specimen [2].

The development of the S-N (σ-N) curve based fatigue design triggered by these early activities was highly important not only for railway applications but for engineering in general [3]. Wohler led to the identification of the fatigue limit for steels. Despite its long use, there is growing evidence that for lives longer than the conventional 10^6 to 10^7 cycles, at which the fatigue limit is determined, the safe stress range continues to be eroded down to 10^9 cycles and more, which is at the very long lives typical of that required of axles and wheels.

Furthermore, Wohler's studies clearly identified the benefits of gradual transitions in profile. He also observed fretting initiated failures due to micro-slip between press fitted wheels and axles [1].

Railway axles are safety critical components whose failure may result in derailments, deaths and injuries. An accident in Versailles, near to Paris, in 1842 was the first railway accident resulting in serious damage. In this accident, the driving axle of a four-wheel locomotive was broken suddenly with the resulting death of 100 people. Another accident that led to derailment was the broken axle of a train moving at 80 km/h in Sheffield, United Kingdom in 1884. Twenty-four people lost their lives [2]. Hoddinott examined the accidents related to axle failures taking root from mechanical loads, electrical arcing and corrosion in his article. For instance, an accident at Rickerscote in 1996 was reported as a complete fracture of an axle and consequent derailment of a two-axle freight wagon containing liquid carbon dioxide. The derailed wagons blocked the adjacent line and were run into by a traveling post office train going in the opposite direction. One person was killed and there were 10 injuries. After technical examination of broken axle, it was clear that the corrosion pitting increased

† This paper was recommended for publication in revised form by Associate Editor Jooho Choi

*Corresponding author. Tel.: +90 212 383 2883, Fax.: +90 212 261 6659
E-mail address: mbarut@yildiz.edu.tr

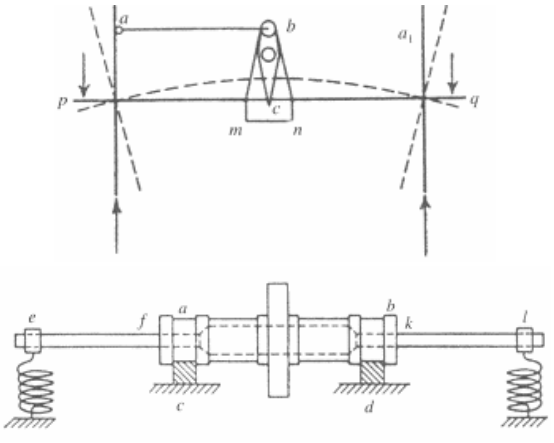

Fig. 1. Wohler's apparatus fatigue testing machine [2].

the stress locally in the axle to initiate a fatigue crack. The crack then grew and the axle finally broke into two pieces. Those accidents accelerated investigations on axles in the UK, and special axles have been started to be designed [4]. Also, it is possible to see European Community Standards for axle design in the paper of Snell [5]. Also, Hirakawa et al. [6] analyzed the causes of failure in railway axles to show how the results have been applied to improve axle manufacture and in-service inspection. They also compared the axles used in Europe and Japan for fatigue design method. Dedmon et al. presented the results of stress analysis calculations that were performed for various different North American freight railroad axle designs [7]. They proposed that a standard axle stress analysis method be adopted by the North American freight railway industry for new axle designs. Baretta et al. emphasized that in spite of the criticality of axles, modern approaches have not been used in addressing a critical revision of traditional design [8]. They studied the scale effects in fatigue limit and in crack growth rate for high strength steel used for high speed railway axles.

Gerdun et al. examined two cases of failures in axles and cylindrical roller bearings of a freight wagon servicing for about 30 years. The examination has proven that the failures were caused by fatigue fractures of the inner rings of the bearings. Dynamic strength of bearings was exceeded, then the rings widened and the axle slid in them. Finally, the axle-box housing deformed and breaking occurred [9]. Vogwell also studied the failed wheel-drive shaft component used on an unmanned, remotely operated vehicle for maneuvering military targets. This study showed how vulnerable such a rotating component can be to failure by fatigue [10]. Stitchel and Knothe presented a method of a fatigue life prediction for railway vehicles based on computer simulation [11]. They evaluated stresses in certain bogie cross sections by knowing the forces and predicted the fatigue life by using a cumulative damage theory. Chen and Xiong presented a design-driven validation approach. They employed a Bayesian approach combining data from both physical experiments and the computer model, to develop a prediction model as the replacement of the original computer model for the purpose of design [12]. Also, McDonald and Mahadevan presented a single-loop reliability design optimization formulation based on first-order reliability method and an equivalent formulation that can also include system-level reliability constraints [13]. Guclu and Metin presented a physical model in the form of a 22-degrees-of-freedom half light rail transport vehicle and differential equations created for analyzing vibrations. They realized a computer simulation to minimize displacement and acceleration of the vibrations obtained in the end of simulations based on time and frequency domains. Then, they carried out a fuzzy logic controller to control vibrations in the simulation environment [14].

Furthermore, researchers are not only dealing with axles, but also there is a wide range of interest in the other components of rail vehicles. For instance, many designs can improve the critical speed such as the implementation of elasto-damper-coupled-wheel sets in conventional rail vehicles. Lieh and Yin studied the stability of an elastic wheel set coupled with torsional spring and damper [15]. With flexible elements between two wheels, the critical speed regions for both constant and time-varying models have been determined. Mathematical modeling and simulation of train dynamic behavior has also been useful for better understanding of conditions leading to derailment. Durali and Shadmehri studied train derailment and hunting in severe braking conditions. They solved different car weight configurations when severe braking is applied. They determined optimum configuration of cars in a light heavy set, and critical derailment velocity to minimize the tendency of train derailment [16]. The vehicle response for earthquake disasters is another important subject for researchers. It is beneficial for the system safety to study dynamic stability and the possibility of derailment directly caused by the track excitations of great earthquakes. Nishimura and friends have developed a new vehicle dynamics simulation with unique modeling specifically taking account of internal slide forces between the vehicle body and the bogie resulting from large motions of vehicles [17]. Also, Lee and Cheng have proposed a new dynamic model of railway vehicle moving on curved tracks based on the heuristic non linear creep model [18].

The reason for need to examine axles arises because of their safety critical nature. They have been subjected to large numbers of repeated loading cycles. Each time that the axle rotates, an element of material on the surface of the axle goes from a compressive state to a tension state of equal magnitude. Reasons such as loading geometry, surface quality, corrosion effect, material failure, being heterogeneous of micro structure, lead to local stress accumulation on components. A failure crack begins from the regions including these stress accumulations. Then it moves ahead and finally the break occurs--called fatigue fracture. Also, instead of maximum stress values, the periodic variation (load cycle) of stress becomes important.

The objective of the present paper is to review and analyze the causes of failure in the railway axle. First, the problem is

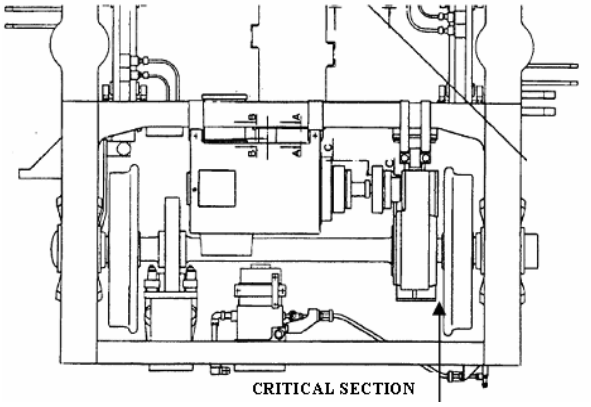

Fig. 2. Bogie of the rail vehicle.

Fig. 3. The derailment resulting from the broken axle in the accident in Istanbul Esenler train station, 2007.

introduced. The life equations are derived by using equivalent stress, and then S-N diagrams are plotted for displaying the lives versus stress for desired failure percents.

2. Fracture of railway axles

Failures of axles on vehicles that failed in service are described in this section with photographs of the surfaces of the axles and the fracture faces. The dates of axle failures, vehicle type (TR: tramcar and LRT: light rail vehicle), and the kilometers that the axles travel are given in the Appendix.

From the beginning of 1997, axle failures have occurred on rail vehicles of the Istanbul Transportation Co. that have been in service for Istanbul city rail transportation.

The solid axle made from 34CrNiMo6 was first broken at 378000 kilometers. The region of the fracture in all failures is the same as shown in Fig. 2. This critical section where the break occurred is the transition part between wheel and gear box. As a result of the analysis and calculation, it is clear that this critical section of the axle has the minimum safety coefficient

Finally, in 2007 after the vehicle entered the station in Istanbul Esenler, the axle of the vehicle broke and the wheel fell between the rail and the switch as a result of fatigue fracture as shown in Fig. 3.

There was no personal injury in this accident through the

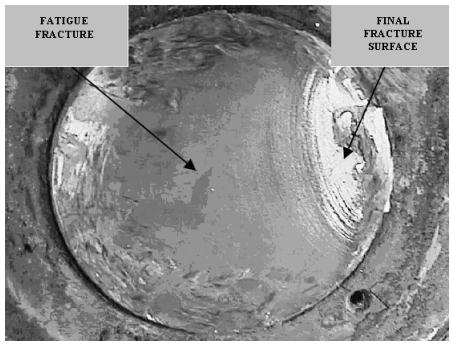

(a)

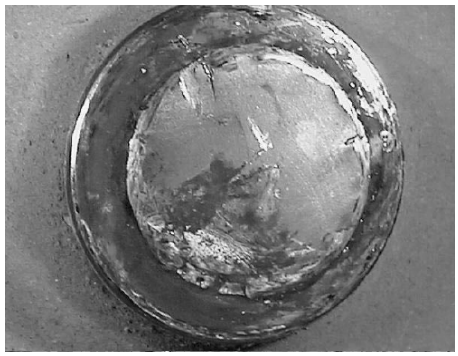

(b)

Fig. 4. The photograph of broken part taken by gear box and wheel [19].

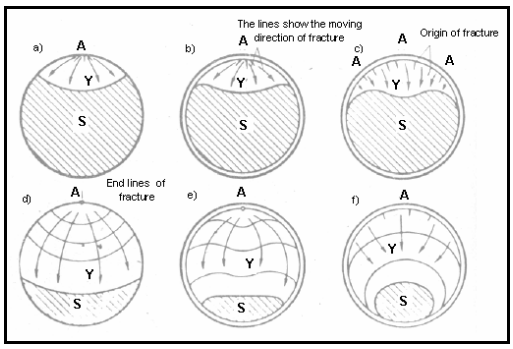

Fig. 5. A-Fracture origins, Y-Fatigue fracture, S-Final fracture surface [19].

low speed. The experts reported that the fracture occurred at the transition section having R6 radius between the wheel and gear box. From the result of examination of fracture surfaces (Figs. 4(a) and 4(b)), it is mentioned that the final fracture surface is 10% less than the total surface. Also, it is clear that two different regions have been detected on surface. While 90 % of the section surface (mat part) has shown the growth of fracture by the time, 10% of the section surface (smooth part) has been pointed out as instantaneously broken [19].

When Fig. 4 and Fig. 5 and are compared, it can be seen that the lines on the fracture surface in Fig. 4 are similar to configurations illustrated at "e" and "f" in Fig. 5. If "e" is accepted as a fracture, the forces affecting the axle are tension and low stress. The edges of the fracture move along rapidly because of the

poor but effective environmental notch impact.

One of the main reasons for preferring rail vehicles as an indispensable transportation system is vehicle and passenger safety. To maintain safety, comprehensive studies are required. The rail vehicle is subject to different passenger number due to different times of the day. Namely, in rush hours passenger number increases while it continues normally in midday. In this study to determine the variable inward loads on an axle and to calculate the equivalent stress for mentioned variable loads and to derive life equations, one of the cumulative failure theories known as Palmgren-Miner method has been used. Cumulative failure theories can be classified as linear and non-linear. It is possible to attain detailed information about these methods from articles of [20-25].

3. Palmigren-Miner theory

Ever since Wohler discussed the railway wagon axle failures in fatigue, this subject gained importance in the design of machinery. The strength of material under the action of completely reversed stress fatigue loads is determined from S-N diagrams. These diagrams are not representative of an actual machine member and therefore the fatigue strength is to be modified to take into account the conditions prevailing for a specific machine subjected to fatigue (Fatemi and Yang [20]).

Fatigue damage increases with applied load cycles in a cumulative manner. Cumulative fatigue damage analysis plays a key role in life prediction of components and structures subjected to field load histories. The first cumulative damage theory was applied by A. Palmgren for predicting the life of roller bearings in 1920 in Sweden. B. F. Langer followed him in general form. However, the theory was not known and used until it occurred in M.A. Miner's study in 1945. Since then, the treatment of cumulative fatigue damage has received increasingly more attention. This linear theory is known as the Palmgren-Miner hypothesis or the linear damage rule [21, 22, 25].

A machine element subjected to variable loads is considered. Operation at a stress level σ_1 gives a life of N_1 cycles. If the element is subjected to n_1, it suffers a damage fraction $D_i = n_i / N_i$. Failure is then predicted to take place where $\sum(n_i / N_i) \geq 1$.

It asserts that the damage fraction at any stress level is linearly proportional to the number of cycles that would produce failure at that stress level. As the element is subjected to a mean stress, the S-N plane is shifted to the location of the applied mean stress level on the fatigue failure surface.

One of the serious drawbacks of this theory is that it does not recognize the order of application of various stress levels and damage is assumed to accumulate at the same rate at a given stress level without a consideration of the past history. Experimental evidence shows that fatigue damage accumulates non linearly, depending on the alternating stress level [23]. If different cyclic stress amplitudes are mixed randomly, Miner's total damage approximates nearly "1". Generally, the use of this theory is satisfactory because the stresses in many applications involve various descents and ascents.

Table 1. Load prediction.

A	B	C	D	E	F	G	H
Full	32	8	35,34	282	314	32000	55550
Medium	32	4		141	173		44975
Low	32	-		-	32		34400

A: Load type
B: Number of seats
C: Person/m^2
D: The area for standing passenger (m^2)
E: Standing passenger number
F: Total passenger number
G: The weight of empty vehicle (kg)
H: Total weight (passenger+vehicle) (kg)

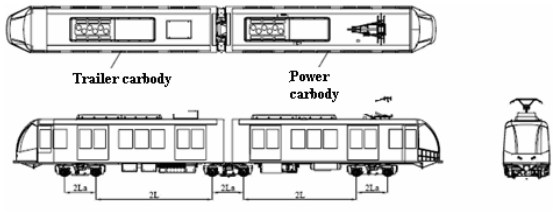

Fig. 6. Layout of the rail vehicle.

$$\frac{n_1}{N_1} + \frac{n_2}{N_2} + \frac{n_3}{N_3} + \ldots + \frac{n_i}{N_i} = K \tag{1}$$

n_1, n_2, …, n_i are load cycles corresponding to σ_1, $\sigma_{2\ldots}$ σ_i . N_1, N_2,…, N_i are lives of elements σ_1, $\sigma_{2\ldots}$ σ_i and K is a constant whose value changes between 0,7 and 2,2. ($0,7 \leq K \leq 2,2$). Also, it is advised to take "1" for the value of K.

To determine the values of n_1, n_2, …, n_i is very difficult. If they are stated as the parts of total life (N_{eq}); $n_1 = c_1.Neq, n_2 = c_2.Neq, \ldots n_i = c_i.Neq$, the following equation where c_1,c_2, …, c_i are proportion factories is derived.

$$\frac{c_1}{N_1} + \frac{c_2}{N_2} + \frac{c_3}{N_3} + \ldots + \frac{c_i}{N_i} = \frac{1}{N_{eq}} \tag{2}$$

4. Fatigue life of railway axles

The vehicle emphasized in this study operates between 06:00 am and 24:00 midnight on the line having 19,95 km. The traveling takes 31 minutes. It is composed of two car bodies (power and trailer bodies) and three bogies with six wheel sets (each wheel set contains two wheels and one axle) as shown in Fig. 6.

To determine the load for an axle, the load prediction, Table 1 is used. The highlighted point in the beginning of the solution is to take into account different occupancy rates (passenger number) during 18 hours (daily performance percent (C) of time is calculated for 18 hours and given in Table 2). Furthermore, the time passing on curves (Table 3), and additional

Table 2. Daily performance percent (C) of load.

	Daily performance percent (C)
Full load	C_{max}=0,33=C_1
Medium load	C_{ort}=0,44=C_2
Low load	C_{min}=0,22=C_3

Table 3. Percents of time of load.

The percent of passing from curve	The percent of passing from level road
$c_1' = 0,487$	$c_2' = 0,513$
$c_1' = 0,365$	$c_2' = 0,635$
$c_1' = 0,731$	$c_2' = 0,269$

The time of one round is 31minutes and total passing time for curves is 5 minutes.

Table 4. Resultant stresses.

Load type	For level road $\sigma_{resultant}$ (N/mm^2)	For curve $\sigma_{resultant}$ (N/mm^2)
Full	176,03*1,25=220,03	295,66*1,25=369,57
Medium	141,85*1,25=177,31	237,6*1,25=297
Low	107,86*1,25=134,82	166,75*1,25=208,43

bending stresses (Table 4) resulting from rolling moments which arise from centrifuge loads are taken to account for calculating equivalent stress and theoretical life. These results are compared with the values given in the Appendix. It is clear that they are similar.

Full load:

$$\frac{1}{\sigma_{eqI}} = \frac{c_1'}{(\sigma_1)_{full\_load/curve}} + \frac{c_2'}{(\sigma_2)_{full\_load/level}} \quad (3)$$

$$\frac{1}{\sigma_{eqI}} = \frac{0,487}{369,57} + \frac{0,513}{220,03}$$

$$\sigma_{eqI} = 274,72 N/mm^2$$

Medium load:

$$\frac{1}{\sigma_{eqII}} = \frac{c_1'}{(\sigma_1)_{medium\_load/curve}} + \frac{c_2'}{(\sigma_2)_{medium\_load/level}} \quad (4)$$

$$\frac{1}{\sigma_{eqII}} = \frac{0,365}{297} + \frac{0,635}{177,31}$$

$$\sigma_{eqII} = 208,03 N/mm^2$$

Low load:

$$\frac{1}{\sigma_{eqIII}} = \frac{c_1'}{(\sigma_1)_{low\_load/curve}} + \frac{c_2'}{(\sigma_2)_{low\_load/level}} \quad (5)$$

$$\frac{1}{\sigma_{eqIII}} = \frac{0,731}{208,43} + \frac{0,269}{134,82}$$

$$\sigma_{eqIII} = 183 N/mm^2$$

Equivalent strain:

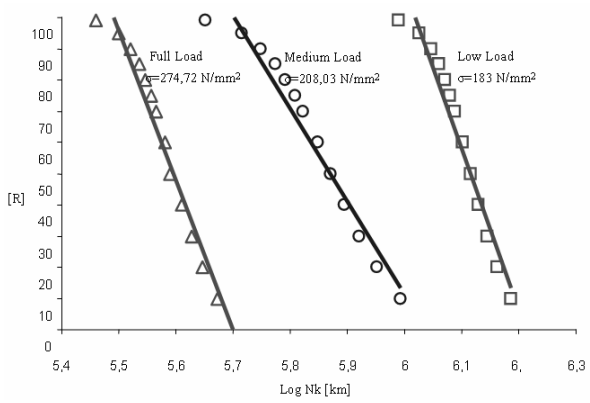

Fig. 7. Reliability-life diagram.

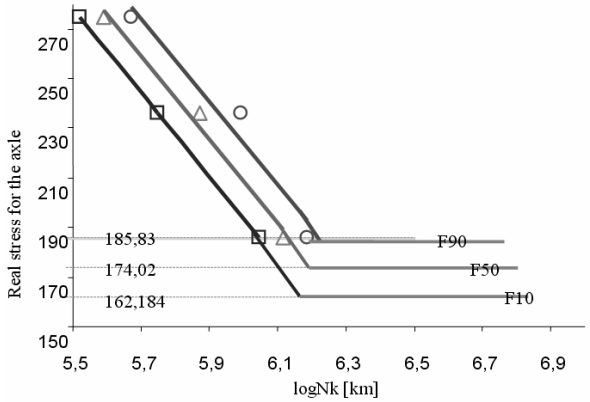

Fig. 8. Stress-life diagram [km].

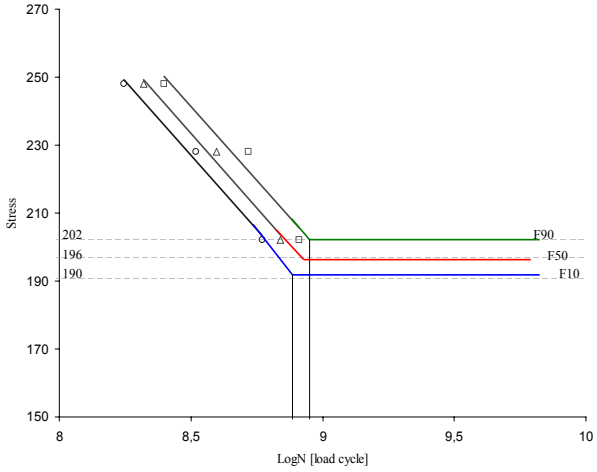

Fig. 9. Stress-life diagram [load cycle].

$$\frac{1}{\sigma_{eq}} = \frac{C_1}{\sigma_{eqI}} + \frac{C_2}{\sigma_{eqII}} + \frac{C_3}{\sigma_{eqIII}} \quad (6)$$

If the values in Tables 2, 3 and 4 are used in the related equations, $\sigma_{eq} = 220$ N/mm^2.

This equivalent stress value is predicated on deriving the life equations for both [km] and [load cycle]. S-N diagrams plot the number of load cycles versus a stress value. In this

study, the logarithmic equations are obtained from the relation between stress and life in the infinite life region. Diagrams are plotted for 10%, 50%, and 90% reliability and failure. Also, it is possible to plot the diagrams for 0,1%…99,9% reliability. The diagrams based on broken axles are presented in Figs. 7-9.

Fig. 7 is the first diagram resulted from evaluation of data given by the firm. In this diagram, it is possible to realize the life values for 0,1%...99,9% reliability of the axle subjected to stress for full, medium or low loads.

In Figs. 8 and 9, the Wohler diagram is plotted for [km] and [load cycle], respectively. It enables one to find the stress values versus at 10%, 50%, 90% failure for the axle made from 34CrNiMo6.

5. Life evaluation of railway axles

In this part, the derived life equations for both 10% and 90% failure are introduced. The curves formed by the mentioned equations are presented in Figs. 10-12. The obtained life values are surely performed lives. It is not possible to get any value under these limits. Also, to predict fatigue failure previously provides avoiding a fracture. There are two kinds of axles mentioned in the table in the Appendix. It is possible to notice the difference from the last two columns. In the first type the axle only runs on the tramcar, and in the second type the axle runs both on the tramcar and light rail vehicle. So this information has been implemented in the calculations.

Derived life equations related to [km] and plotting of stress-life diagram (Fig. 10):

As seen from the diagram, σ_{Kmax}=930N/mm^2 and σ_{Kmin}= 780N/mm^2 for the axle which is made from 34CrNiMo6 material. Also, continuous strength value is 0,44.σ_K for the case of bending [25]. To plot the diagram, the life equations given below are used:

Derived life equation for % 90 failure (F90);

$$\log N_k = 6,4547 - 3,8386\frac{\sigma_g}{\sigma_{K\max}} \tag{7}$$

Derived life equation for % 10 failure (F10);

$$\log N_k = 7,1432 - 4,6036\frac{\sigma_g}{\sigma_{K\min}} \tag{8}$$

It is possible to see that the life of the axle is going to be $10^{4,7658}$ [km] for 90% failure and $10^{5,1177}$ [km] for 10% failure.

Derived life equations related to [load cycle] and plotting of stress-life diagram (Fig. 11):

Derived life equation for % 90 failure (F90);

$$\log N = 10,1515 - 7,9462\frac{\sigma_g}{\sigma_{K\max}} \tag{9}$$

Derived life equation for % 10 failure (F10);`

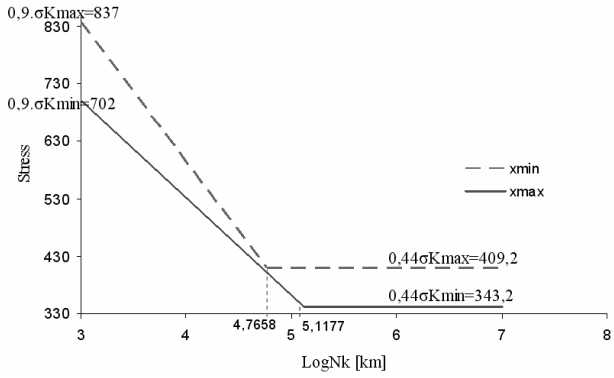

Fig. 10. TR: Stress-life (logNk) [km].

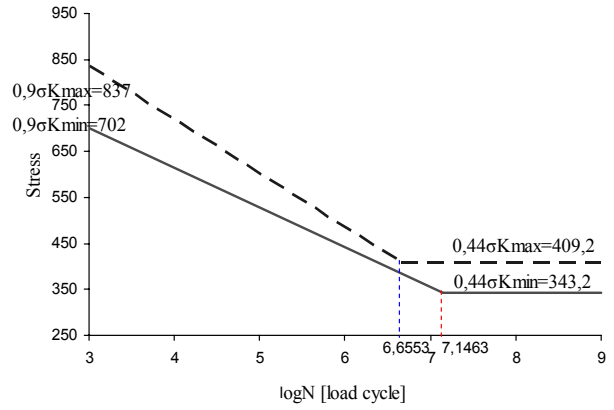

Fig. 11. TR: Stress-life (logN) [load cycle].

$$\log N = 11,1122 - 9,0136\frac{\sigma_g}{\sigma_{K\min}} \tag{10}$$

It is possible to see that the life of the axle is going to be $10^{6,6553}$ [load cycle] for 90% failure and $10^{7,1463}$ [load cycle] for 10% failure.

In Figs. 10 and 12, the unit of X axis is given as life (L) and this equality is given below:

$$L = N_k = \frac{N.Perimeter[m]}{1000} \text{ [km]} \tag{11}$$

In this equation, perimeter=πD_0 [mm] and D_0 is the diameter of the wheel (600mm).

Derived life equations related to [km] and plotting of stress-life diagram (Fig. 12):

Derived life equation for % 90 failure (F90);

$$\log N_k = 6,9663 - 4,4104\frac{\sigma_g}{\sigma_{K\max}} \tag{12}$$

Derived life equation for % 10 failure (F10);

$$\log N_k = 7,6210 - 5,1349\frac{\sigma_g}{\sigma_{K\min}} \tag{13}$$

It is possible to see that the life of the axle is going to be

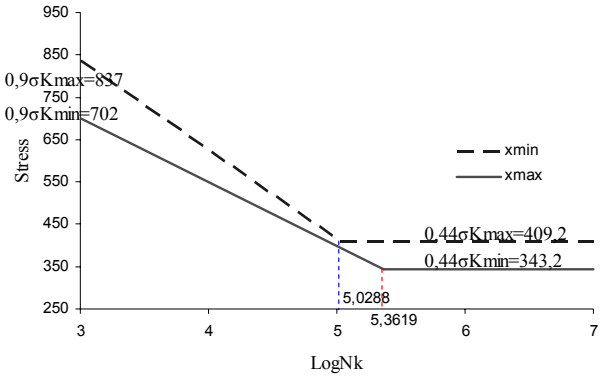

Fig. 12. TR-LRT: Stress-life (LogNk) [km].

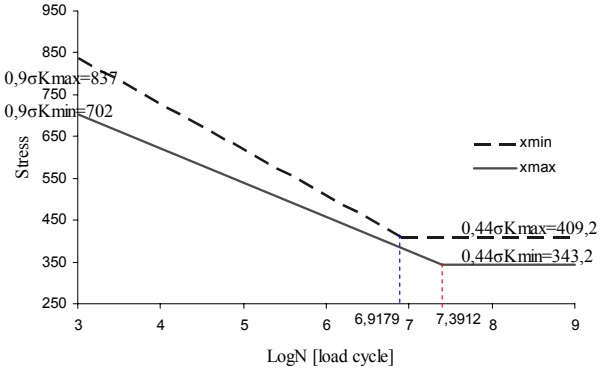

Fig. 13. TR-LRT: Stress-life (LogNk) [load cycle].

$10^{5,0288}$ [km] for 90% failure and $10^{5,3619}$ [km] for 10% failure.

Derived life equations related to [load cycle] and plotting of stress-life diagram (Fig. 13):

Derived life equation for % 90 failure (F90);

$$\log N = 10,6653 - 8,5171\frac{\sigma_g}{\sigma_{K\max}} \tag{14}$$

Derived life equation for % 10 failure (F10);

$$\log N = 11,5913 - 9,546\frac{\sigma_g}{\sigma_{K\min}} \tag{15}$$

It is possible to see that the life of the axle is going to be $10^{6,9179}$ [load cycle] for 90% failure and $10^{7,3912}$ [load cycle] for 10% failure.

The life values obtained from the numerical evaluations confirm the statistical evaluation for 10% and 90% failure.

The error analysis (HR) is performed as below:

$$H_R = \frac{N_{REAL} - N_{CALCULUS}}{N_{REAL}} \tag{16}$$

The error rate is calculated as 4% for 90% failure and 8% for 10% failure in [km] terms. The error rate is calculated as 0,5% for 90% failure and 1% for 10% failure in [load cycle] terms.

6. Conclusions

The fractures of axles that have occurred at the Istanbul Transportation Co. are examined. It is clear that the fractures result from fatigue according to the "LRT Axle Report" prepared by the establishment under the responsibility of the firm.

The rail vehicle is subjected to different occupancy rates at the different times during the day. So, it leads to handle the situation for three loading configuration; full, medium and low load.

The additional stress resulting from curving and the time passing from the curves have also been considered for determining the equivalent stress in the solution by using Palmgren-Miner cumulative life theory. In light of the foregoing what the life of the axle will be related to the reliability percent (0,1%...99,9%) could be realized from the plotted diagrams by the firm. In other words, it is understood at which stress an axle could reach reliability at any
percentage (%).

The Wohler diagrams depending on [km] and [load cycle] are plotted individually by the help of the stress values corresponding to 10%, 50%, 90% failure values. Also, the diagrams provide to determine the life values corresponding to 10%, 50%, 90% failure in the time-bound and continues strength regions.

The list in the Appendix explains that some of axles have run at TR and some of them have run both at TR and LRT. So, for 10% and %90 failures, the stress values and life values could be read from the diagrams by discussing the conditions of TR and TR-LRT. The required equations for performing the diagrams are derived on our part. Finally, the error analyses are performed.

Acknowledgment

This work was supported by Istanbul Transportation Co., Turkey. The authors would also like to thank Istanbul Transportation Co. for providing the data and reports.

Nomenclature

TR : Tramcar
LRT : Light rail vehicle
R : Reliability
F : Failure
N : Life
n : Load cycle
c : Proportion factor
σ : Stress
H_R : Error

References

[1] R. A. Smith, Railway fatigue failures: an overview of a long standing problem, *Mat.-wiss. U. Werkstoffiech*. 36 (11) (2005).

[2] R. A. Smith and S. Hillmansen, A brief historical overview of the fatigue of railway axles, *Proc. Inst. Mech. Engn. Part E, J. Rail and Rapid Transit,* 218 (2004).
[3] U. Zerbst, K. Madler and H. Hintze, Fracture mechanics in railway applications-an overview, *Engineering Fracture Mechanics*, 72 (2005) 63-194.
[4] D. S. Hoddinott, Railway axle failure investigations and fatigue crack growth monitoring of an axle*, Proc. Inst. Mech. Engn. Part E J. Rail and Rapid Transit*, 215 (2004).
[5] J. R. Snell, Key issues in the application of unified railway axle standards, *Proc. Inst. Mech. Engn. Part E J. Rail and Rapid Transit*., 218 (2004).
[6] K. Hirakawa, K. Toyama and M. Kubota, The analysis and prevention of failure in railway axles, *Int. Journal Fatigue*, 20 (1998) 135-144.
[7] S. L. Dedmon, J. M. Pilch and C. P. Lonsdale, A comparison of railroad axle stress results using different design sizes, loading criteria and analysis method, *Proceedings of 2001 ASME International Mechanical Engineering Congress and Exhibition*, New York, NY, USA, (2001), November 1-16.
[8] S. Baretta, A. Ghidini and F. Lombardo, Fracture mechanics and scale effects in the fatigue of railway axles, *Engineering Fracture Mechanics*, 72 (2005) 195-208.
[9] V. Gerdun, T. Sedmak, V. Sinkovec, I. Kovse and B. Cene, Failures of bearings and axles in railway freight wagon, *Engineering Failure Analysis,* 14 (2007) 884-994.
[10] J. Vogwell, Analysis of a vehicle wheel shaft failure, *Engineering Failure Analysis*, 5 (4) (1998) 271-277.
[11] S. Stichel and K. Knothe, Fatigue life prediction for an S-train bogie, *Vehicle System Dynamics Supplement,* 28 (1998) 390-403.
[12] W. Chen and Y. Xiong, A design-driven validation approach using Bayesian prediction models, *Journal of Mechanical Design, ASME,* 130 (2008).
[13] M. McDonald and S. Mahadevan, Design optimization with system-level reliability constraints, *Journal of Mechanical Design*, *ASME*, 130 (2008).
[14] R. Guclu and M, Metin, Fuzzy logic control of vibrations of a light rail transport vehicle in use in Istanbul traffic, *Journal of Vibration and Control*, 15 (9) (2009) 1423-1440.
[15] J. Lieh and J. Yin, Stability of a flexible wheelset for high speed rail vehicles with constant and varying parameters, *Journal of Vibration and Acoustics, ASME*, 120 (1998) 997-1002.
[16] M. Durali and B. Shadmehri, Nonlinear analyses of train derailment in severe braking, *Journal of Dynamic Systems, Measurement, and Control, Transactions of the ASME*, 125 (2003) 48-53.
[17] K. Nishimura, Y. Terumichi, T. Morimura and K. Sogabe, Development of vehicle dynamics simulation for safety analyses of rail vehicles on excited tracks, *Journal of Computational and Nonlinear Dynamics, Transactions of the ASME*, 4 (2009).
[18] S.-Y. L ee and Y.-C. Cheng, A new dynamic model of high-speed railway vehicle moving on curved tracks, *Journal of Vibration and Acoustics*, ASME, 30 (2008).
[19] LRT Axle Report-Edited by Ergul Cankaya, Istanbul Transportation Co., (2005).
[20] A. Fatemi and L. Yang, Cumulative damage and life prediction theories: a survey of the state of the art for homogeneous materials, *Int. Journal of Fatigue*, 20 (1) (1998) 9-34.
[21] G. E. Saatci and N. Tahrali, Cumulative failure theories and life evaluation for fatigue crack, *Journal of Aeronautics and Space Technologies*, 1/2 (2003[1]) 33-39.
[22] G. E. Saatci and N. Tahrali, Cumulative failure theories and the application to transmission elements, *Journal of Aeronautics and Space Technologies,* 1 (2003[2]) 21-30.
[23] G. E. Saatci, The examination of cumulative failure theories for dynamic fractures and application to transmission elements of GTD model 4×4 military vehicle, PhD thesis, Yildiz Technical University, (2002).
[24] J. S. Rao, A. Pathak and A. Chawla, Blade life: a comparison by cumulative damage theories, *Journal of Engineering for Gas Turbines and Power, Transactions of the ASME*, 123 (2001) 886-892.
[25] N. Tahrali and F. Dikmen, Reliability and life calculations for machine elements, Yildiz Technical University Press, (2004).

Appendix

A : Ultrasonic inspection period
B : Vehicle no
C : Date
D : Km
E : Where the failure has occurred (TR/LRT)
F : Where the axle has run before

Life [km] values table taken from Istanbul Trans. Co.

A		B	C	D	E	F
LRT 100.000 Km	TR 18.000 Km	513	08.06.1997	378.800	TR	TR
		529	22.08.1997	360.000	TR	TR
		532	25.11.1997	380.000	TR	TR
		533	24.03.1998	390.167	TR	TR
		557	14.09.1998	332.761	TR	TR
		514	11.10.1998	446.000	TR	TR
		517	12.05.1999	507.500	TR	TR
		513	08.06.1999	499.064	TR	TR
		517	11.11.1999	543.750	TR	TR
		526	14.12.1999	545.630	TR	TR
		529	26.10.2000	571.701	TR	TR
		530	04.01.2001	622.000	TR	TR
		105	18.04.2001	510.300	TR	TR
		536	03.09.2002	1.032.000	LRT	LRT
LRT 30.000Km	TR 18.000	504	07.02.2003	761.000	TR	TR
		503	06.10.2003	821.000	TR	TR
		101	24.12.2004	612.525	LRT	TR

		561	16.03.2005	1.289.000	LRT	TR
		560	06.05.2005	1.291.000	LRT	TR
		101	20.05.2005	659.708	LRT	TR
LRT 10.000 Km	TR 6.000 Km	530	24.05.2005	866.500	LRT	TR
		558	24.05.2005	813.500	LRT	TR
		131	24.05.2005	1.234.377	LRT	TR
		107	16.06.2005	1.261.298	LRT	TR
		525	06.09.2005	901.279	LRT	TR
		520	21.09.2005	871.800	LRT	TR
		520	21.09.2005	871.800	LRT	TR
		111	02.12.2005	1.276.400	LRT	TR
		556	07.02.2006	1.404.655	LRT	TR
		514	24.02.2006	879.239	LRT	TR
		560	05.05.2006	1.391.275	LRT	TR
		517	26.07.2006	950.000	LRT	TR
		107	09.11.2006	1.471.441	LRT	TR
		565	06.01.2007	1.501.000	LRT	TR
		116	12.01.2007	1.443.922	LRT	TR
		555	12.01.2007	1.485.698	LRT	TR
		111	15.01.2007	1.381.371	LRT	TR
		111	25.01.2007	1.384.576	LRT	TR
		507	29.01.2007	861.627	LRT	TR
		507	29.01.2007	861.627	LRT	TR
		510	19.04.2007	859.917	LRT	TR
		503	17.05.2007	893.314	LRT	TR
		132	31.05.2007	1.439.114	LRT	TR
		523	04.07.2007	1.000.286	LRT	TR
		505	15.08.2007	945.487	LRT	TR
		524	19.09.2007	1.256.356	LRT	TR
		520	04.09.2007	1.082.673	LRT	TR

Meral Bayraktar has been working at Yildiz Technical University Mechanical Engineering Department since 2001. She has been studying on machine elements, mechanical vibrations and rail vehicle dynamics.

Necati Tahrali has been working at Yildiz Technical University Mechanical Engineering Department since 1970. His research area is about machine elements, machine dynamics and mechanical vibrations. He studied strength, life and reliability analysis of gear mechanisms at Munih Technic University Gear Mechanism Research Laboratory (Technische Universitaet München-Almanya, Forschungsstelle für Zahnraeder und Getriebebau FZG).

Rahmi Guclu has been working at Yildiz Technical University Mechanical Engineering Department since 1987. His research interests include mechanical vibrations, system dynamics and control, vehicle dynamics, structural vibrations and rail system dynamics.